Computational Studies of the Chemistry of Syn Acetaldehyde Oxide

Keith T. Kuwata,*,† Kristen L. Templeton,† and Alam S. Hasson‡

Department of Chemistry, Macalester College, Saint Paul, Minnesota 55105-1899 and Department of Chemistry, California State University, Fresno, California 93740-8034

Received: June 17, 2003; In Final Form: September 11, 2003

Syn carbonyl oxides generated in alkene ozonolysis have been implicated as sources of hydroxy radical (•OH) in the atmosphere. We report quantum chemical calculations at the B3LYP/6-31G(d,p), CBS-QB3, MPW1K/6-31+G(d,p), and CBS-APNO levels to characterize the reactivity of syn acetaldehyde oxide and its vinyl hydroperoxide isomer. The vinoxy radical formed upon vinyl hydroperoxide decomposition is converted to a chemically activated peroxy radical in the presence of O_2. All methods besides MPW1K predict that this species undergoes a 1,4-hydrogen shift with an activation barrier of ∼20 kcal/mol and then decomposes to yield •OH. RRKM/Master equation calculations predict that this unimolecular reaction of the peroxy radical will compete significantly with its collisional stabilization even up to 1 atm pressure. This chemistry can partly account for the •OD radicals recently observed in the ozonolysis of alkenes with vinylic deuteriums. The CBS-QB3 and CBS-APNO methods predict relative energies that agree to within ±1 kcal/mol for most of the reactions considered in this study. The B3LYP/6-31G(d,p) and MPW1K/6-31+G(d,p) predictions are considerably less precise and often disagree with the model chemistry predictions.

I. Introduction

The reaction of ozone with alkenes (or ozonolysis) has enjoyed renewed attention in recent years because of convincing evidence[1−4] that this reaction can function as a nonphotochemical source of hydroxy radical (•OH) in the troposphere. Alkene ozonolysis can therefore significantly impact the oxidative strength of the lower atmosphere not only at night, but also during daylight hours over urban and heavily forested areas characterized by high alkene mixing ratios.

We understand some of the factors that affect the yield of •OH in the ozonolysis of a given alkene. One such factor is the conformation of the carbonyl oxides produced. Recent studies suggest that carbonyl oxides with allylic hydrogens syn to the terminal oxygen will produce •OH, but not carbonyl oxides with allylic hydrogens only anti to the terminal oxygen.[5−13] Quantum chemistry has provided a rationale for these generalizations.

Specifically, previous theoretical studies[8,9] have predicted that syn carbonyl oxides preferentially undergo a 1,4-hydrogen shift to form vinyl hydroperoxides (Reaction 1). The alternative pathway, closure to the dioxirane (Reaction 2), has an activation barrier 7−9 kcal/mol higher in energy.

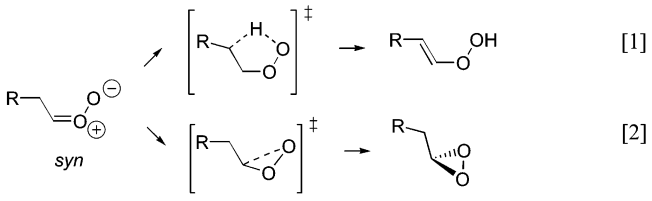

The vinyl hydroperoxides are usually assumed to decompose promptly to afford •OH (Reaction 3). However, several ozonolysis studies over the decades[11,14−17] have reported observing α-hydroxycarbonyls and have attributed their formation to the isomerization of the vinyl hydroperoxide (Reaction 4). Some[18] have identified this species as the •OH precursor in ozonolysis.

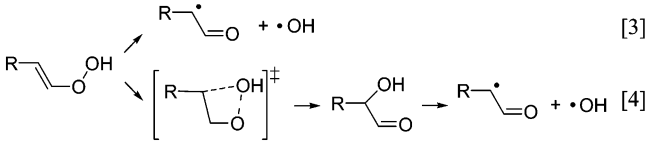

In this paper, we provide computational evidence against this mechanism of α-hydroxycarbonyl formation.

Previous quantum chemical studies have predicted that anti carbonyl oxides preferentially close to dioxiranes (Reaction 5).[8−10] The alternative pathway, a 1,3-hydrogen shift that gives an acyl radical and •OH (Reaction 6), has an activation barrier 12−14 kcal/mol higher in energy.

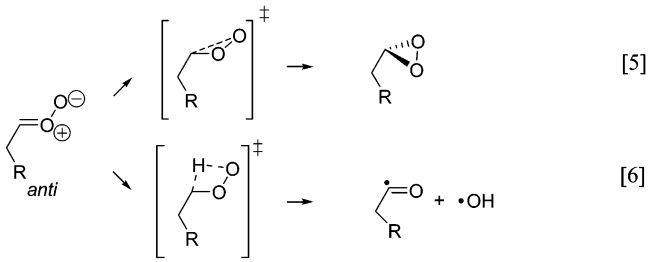

Workers have therefore generally assumed[5,8,9,12,13,19] that the anti form cannot serve as a •OH precursor.

However, Kroll et al.[20] have recently challenged this assumption on the basis of experiments with *cis*- and *trans*-3-hexene both deuterated at the vinylic positions. The ozonolysis of such alkenes will produce carbonyl oxides with D's in a 1,3-relationship to the terminal oxygen:

* Corresponding author. E-mail: kuwata@macalester.edu.
† Macalester College.
‡ California State University, Fresno.

10.1021/jp035720h CCC: $25.00
Published on Web 11/26/2003

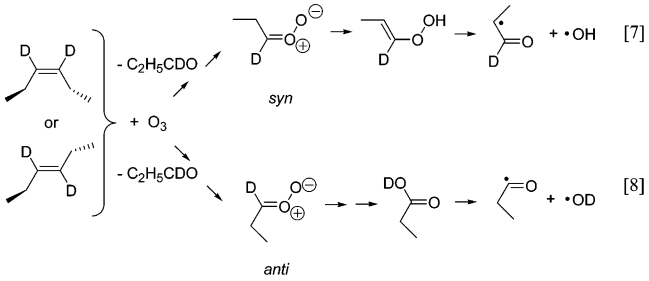

[7]

[8]

Since these deuteriums cannot participate in 1,4-shifts, no •OD should be observed. However, Kroll et al.'s LIF measurements indicate that from 10 to 35% of the hydroxy radicals produced are deuterated. The authors propose that anti carbonyl oxides will isomerize to carboxylic acids and then decompose to afford the observed •OD radicals (Reaction 8). Quantum chemistry predicts[21] that isomerization to the acid has an activation barrier of only 2 kcal/mol and will be exothermic by −115 kcal/mol. The homolytic cleavage of the C−OD bond in the vibrationally "hot" acid, which requires 110 kcal/mol,[22] is therefore possible thermodynamically.[5,23] However, there is no direct experimental evidence for such a pathway, and other unimolecular pathways have lower activation enthalpies.[21] In addition, much of the acid should be collisionally stabilized, with some fraction then undergoing bimolecular reaction.

We suggest that vinoxy radicals, which are co-generated with •OH in vinyl hydroperoxide decomposition (Reaction 7), are another important source of •OD radicals in Kroll et al.'s[20] experiments. First, note that vinylic deuteriums in the alkene starting material will end up at the aldehydic position in these radicals. Second, there is spectroscopic evidence[24,25] that the reaction of vinoxy with O_2 produces hydroxy radical. We provide rigorous quantum chemical evidence that this •OH/•OD arises from an intramolecular abstraction at the aldehydic position:

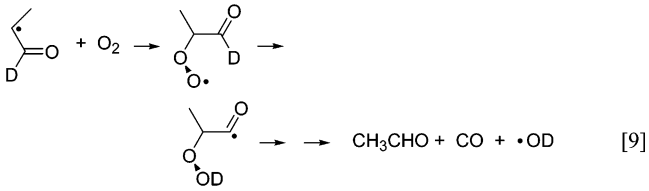

[9]

Our proposal is that in the presence of O_2, syn carbonyl oxides can function both as primary and secondary sources of hydroxy radical.

II. Theoretical Methods

All minima and transition structures for the reactions under consideration were located first by density functional theory with the B3LYP functional[26] and the 6-31G(d,p) basis set.[27,28] The nature of each stationary point was determined by calculating harmonic vibrational frequencies. Each minimum we report has all real frequencies, and each transition structure has one imaginary frequency. Animation of the imaginary frequency, sometimes combined with intrinsic reaction coordinate (IRC) calculations, enabled us to associate a given transition structure unequivocally with its reactant and product. Singlet diradical species were treated with broken spin symmetry wave functions. The geometry and vibrational frequencies of each minimum and transition structure were then recomputed at the B3LYP/6-311G(2d,d,p) level for use in CBS-QB3 calculations.[29] The combination of geometries largely unaffected by spin contamination[30] and high-level single-point calculations should make the CBS-QB3 model chemistry an accurate method for both minima and transition structures.

TABLE 1: Predictions for Reaction 10 (Relative Energies in kcal/mol; Bond Lengths in Å)

	energies (Relative to **1**)		geometry of **TS2**	
	2	**3**	*r*(C---H)	*r*(H---O)
B3LYP[a]	+15.4	−16.3	1.339	1.366
CBS-QB3[b]	+17.1	−18.7	1.339	1.373
MPW1K	+16.3	−19.1	1.317	1.356
CBS-APNO[c]	+16.9	−16.9	1.336	1.345

[a] These values have previously been reported by Cremer and co-workers.[9] [b] Uses B3LYP/6-311G(2d,d,p)-optimized geometries. [c] Uses QCISD/6-311G(d,p)-optimized geometries.

However, B3LYP, which has been employed in many of the recent mechanistic studies of ozonolysis,[5,8,9,12,13,21,31] has been reported[32−37] to underestimate activation barriers because of errors both in geometry and energy. This problem is particularly acute for hydrogen-shift reactions, which as discussed above, play a critical role in the mechanism of •OH production in ozonolysis. We therefore tested the B3LYP/6-31G(d,p) and CBS-QB3 energetics for all reactions with both the MPW1K/6-31+G(d,p) density functional method, parametrized by Truhlar and co-workers[33,34] to reproduce reliably known hydrogen-shift reaction barriers, and the CBS-APNO model chemistry,[38] a computationally demanding but highly reliable procedure[39] which uses QCISD/6-311G(d,p)-optimized geometries.[40] All relative energies reported have been corrected for differences in zero-point vibrational energy, scaled by 0.963 for B3LYP/6-31G(d,p),[8] 0.99 for B3LYP/6-311G(2d,d,p),[29] 0.9515 for MPW1K/6-31+G(d,p),[34] and 0.9251 for the HF frequencies employed by CBS-APNO.[38] All calculations were performed with the Gaussian 98 suite of programs.[41]

III. Results and Discussion

A. Syn Acetaldehyde Oxide Rearrangements. Our calculations focus on the chemistry of syn acetaldehyde oxide as a model for the syn propanal oxide generated in Kroll et al.'s[20] experiments. Table 1 summarizes our predictions for the carbonyl oxide **1**/vinyl hydroperoxide **3** isomerization:

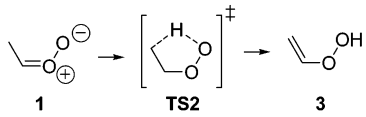

[10]

The four methods agree to within ±1 kcal/mol for the forward barrier and to within ±2 kcal/mol for the reverse barrier and predict breaking/forming bond lengths in transition structure **TS2** that agree to within ±0.01 Å. The B3LYP/6-31G(d,p) predictions for this reaction agree rather well with the predictions of more rigorous methods, as previously reported by Cremer and co-workers.[8,9]

Tables 2−4 and Figures 1 and 2 present our results for the reactions involving the parent vinyl hydroperoxide **3**:

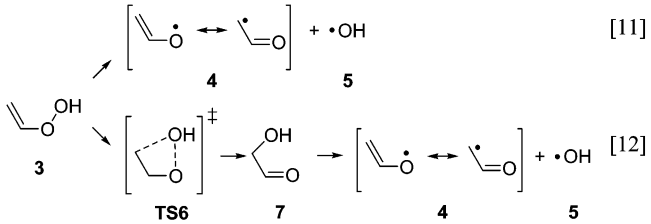

[11]

[12]

TABLE 2: Energetics for the Reactions of Vinyl Hydroperoxide 3 (Relative Energies in kcal/mol)

	3	4+5	TS6a[a]	TS6b[a]	7
B3LYP	0.0	+18.4	+45.0	+38.1	−64.8
CBS-QB3	0.0	+21.0	+27.0	+28.0	−66.8
MPW1K	0.0	+9.5	+58.5	+47.2	−69.6
CBS-APNO	0.0	+20.1	+24.8	+26.8	−67.2

[a] We located two 1,3-sigmatropic shift transition structures (see Figure 2 and the text).

TABLE 3: ΔH°_{298} Values (kcal/mol) for the Reactions in Scheme 1

	reaction number		
	11	13	14
B3LYP	19.6	107.6	41.3
CBS-QB3	22.2	110.6	45.6
MPW1K	10.7	105.6	31.9
CBS-APNO	21.4	109.8	44.6
experiment[a]		109.9 ± 0.8	45 ± 1

[a] Reference 22.

TABLE 4: Breaking and Forming Bond Lengths (in Å) for the 1,3-Sigmatropic Shift Transition Structures in Reaction 12

	geometry of **TS6a**		geometry of **TS6b**	
	r(O---O)	*r*(O---C)	*r*(O---O)	*r*(O---C)
B3LYP	2.212	2.545	2.026	2.396
CBS-QB3[a]	2.216	2.555	2.033	2.415
MPW1K	2.140	2.496	1.977	2.373
CBS-APNO[b]	2.268	2.889	2.134	2.646

[a] Uses B3LYP/6-311G(2d,d,p)-optimized geometries. [b] Uses QCISD/6-311G(d,p)-optimized geometries.

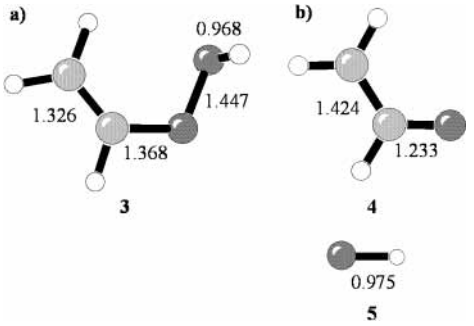

Figure 1. Structures of (a) the vinyl hydroperoxide and (b) the vinoxy and hydroxy radicals. Bond lengths (in Å) computed at the B3LYP/6-311G(2d,d,p) level. Note that in all these figures, gray represents carbons, black represents oxygens, and white represents hydrogens.

All methods besides MPW1K predict that homolysis of the O−O bond in **3** to form **4** and **5** (Reaction 11) requires ∼20 kcal/mol (Table 2). We also predict that this dissociation proceeds without an enthalpic barrier along the reaction coordinate, which is typical for such reactions. These predictions agree with previous studies.[8,9,42] The weakness of the peroxy bond (compared to that in, say, methyl peroxide, whose peroxy bond energy is 45 kcal/mol[22]) is a consequence of resonance stabilization in the vinoxy (•CH_2CHO) radical. As shown in Figure 1, the predicted C−O bond length in •CH_2CHO (**4**) is 0.14 Å shorter than in the hydroperoxide (**3**). This carbon−oxygen double-bond character indicates that the unpaired electron density in vinoxy is largely localized on the β-carbon atom. This is consistent with both microwave spectroscopy studies[43] and previous ab initio calculations[44] on the radical's ground electronic state.

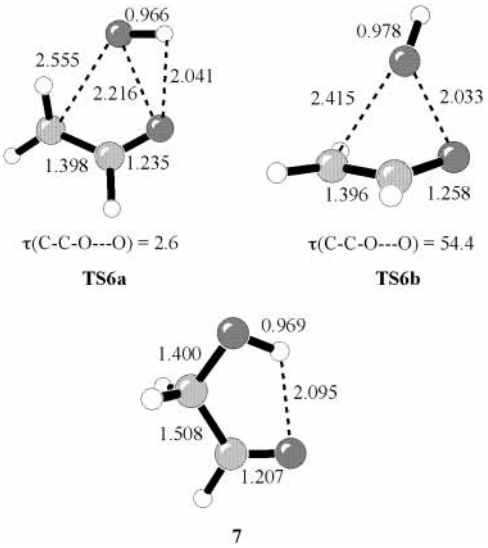

Figure 2. Transition structures (**TS6a** and **TS6b**) for the 1,3-sigmatropic shift of −OH in the vinyl hydroperoxide, and structure of the hydroxyacetaldehyde product (**7**). Bond lengths (in Å) and torsional angles (in degrees) computed at the B3LYP/ 6-311G(2d,d,p) level.

The ∼10 kcal/mol discrepancy in the MPW1K result may reflect a systematic error in this method's treatment of radicals. To test this hypothesis, we computed 298 K reaction enthalpies for the following reactions, comparing ΔH°_{298} values for [13] and [14] with experimental data (Table 3):[22]

SCHEME 1

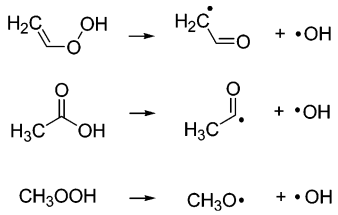

As compared to experiment, MPW1K underestimates the C−O bond enthalpy in acetic acid (Reaction 13) by 4 kcal/mol, and underestimates the O−O bond enthalpy in methyl peroxide (Reaction 14) by 13 kcal/mol. B3LYP underestimates these bond enthalpies by 2−4 kcal/mol. Both density functional methods therefore appear to overestimate the stability of these radicals. In contrast, both CBS-QB3 and CBS-APNO reproduce the experimental bond enthalpies within their uncertainties.

Formation of hydroxyacetaldehyde **7** (Reaction 12) is predicted to be exothermic by −65 to −70 kcal/mol (Table 2). Species **7** contains an intramolecular hydrogen bond (Figure 2) which stabilizes it by 6 kcal/mol, according to our CBS-QB3 calculations. Our calculations reveal two concerted transition states for this 1,3-sigmatropic shift reaction. The two transition structures (Figure 2) involve the in-plane (**TS6a**) and out-of-plane (**TS6b**) motion of the −OH group. An analogous pair of transition structures has recently been reported for the 1,3-shift of $-NH_2$ in allylamine.[45] Steric interactions between the vinoxy moiety and the lone pairs on •OH lead to unusually long breaking and forming bonds in both structures, and the bond lengths in both moieties are similar to those of the individual radicals (Figure 1b). In **TS6a**, there is a hydrogen bond between the •OH and the O of the vinoxy moiety. However, this stabilizing interaction is offset by greater steric repulsion between the two moieties, as is reflected by breaking/forming bond lengths that are 0.1−0.2 Å greater in **TS6a** than in **TS6b**.

TABLE 5: Energetics for the Reactions of the Vinoxylperoxy Radical 10 (Relative Energies in kcal/mol)

	4+8	TS9	10	TS11	12	TS13	14+15	TS16+15	17+5+15	TS18	19
B3LYP	+18.7	+21.1	0.0	+20.4	+6.7	+16.5	+15.9	+15.2	−14.7	+40.9	+0.9
CBS-QB3	+22.9	+27.4	0.0	+19.5	+1.7	+12.8	+7.3	+6.7	−26.3	+39.1	-0.7
MPW1K	+18.2	+26.4	0.0	+26.0	+5.7	+20.7	+17.3	+16.5	−16.5	+44.5	+0.8
CBS-APNO	+22.1	+27.1	0.0	+19.4	+2.2	+11.3	+8.3	+6.5	−25.6	+43.5	0.0

The CBS-QB3 and CBS-APNO methods agree that the in-plane transition structure is slightly lower in energy than the out-of-plane transition structure, with the CBS-APNO barriers being only 1−2 kcal/mol lower than the CBS-QB3 barriers (Table 2). This similarity in energy obtains even though the C---O bond lengths predicted at the QCISD/6-311G(d,p) level are up to 0.3 Å longer than those predicted at the B3LYP/6-311G(2d,d,p) level (Table 4). B3LYP and MPW1K predict forward barriers that are 10−32 kcal/mol higher than the model chemistry predictions.

Nevertheless, all methods agree that the direct decomposition of the hydroperoxide to give one equivalent of •OH requires less energy than the formation of hydroxyacetaldehyde via a single transition state. It is true that at the CBS-APNO level Reaction 12 has an energy barrier only 4.7 kcal/mol higher than the endothermicity of Reaction 11, which suggests that Reaction 12 may not be negligible. However, the same method predicts that the 298 K *free*-energy change for Reaction 11 is only +10.7 kcal/mol. In contrast, the 298 K activation free energy for Reaction 12 is predicted to be +26.0 kcal/mol. The direct decomposition of the hydroperoxide to give vinoxy radical and •OH is therefore favored both energetically and entropically.

This conclusion is supported by our recent experimental and computational study[46] of the decomposition of hydroxymethyl hydroperoxide (HMHP):

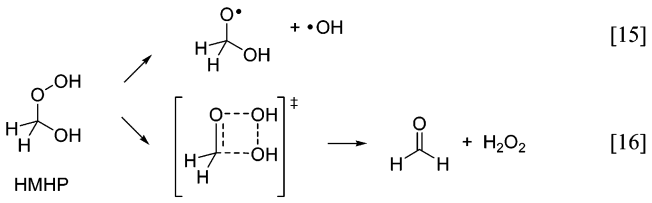

[15] [16]

In ref 46, we predict that Reaction 15 is endothermic by 43.8 kcal/mol, and like Reaction 11, we predict no barrier along the homolysis reaction coordinate. Our predicted activation energy for Reaction 16 is only 4.7 kcal/mol higher than the reaction energy for 15. In ref 46, we also report RRKM/master equation[47] calculations based on our energetics for Reactions 15 and 16. These calculations, which include the effects of entropy, predict Reaction 16 to be negligible compared to Reaction 15.

B. Formation and Isomerization of the Vinoxylperoxy Radical. Table 5 summarizes the energetics for all of the reactions treated in this and the next section.

As discussed above, the unpaired electron in vinoxy radical's ground electronic state is largely localized to the β-carbon. Therefore, O_2 (which is present in both the atmosphere and in ozonolysis experiments) will add preferentially to this atom to give the vinoxylperoxy radical **10** via transition structure **TS9**:

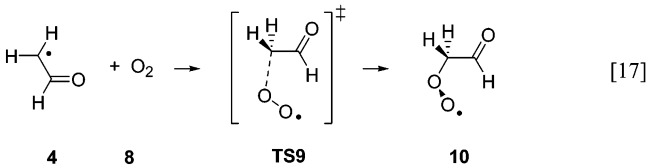

[17]

This reaction has been observed to be relatively facile, with an experimental high-pressure-limit rate constant of $(2-3) \times 10^{-13}$ cm^3 molecule^{-1} s^{-1} at 300 K.[24,25,48]

The four methods we used predict reaction barriers of 2.4−8.2 kcal/mol, with the two model chemistries both predicting barriers of ∼5 kcal/mol. Our predictions are all significantly larger than the barrier of 0.7 kcal/mol determined by Oguchi et al.'s RRKM analysis[49] of Zhu and Johnston's pressure-dependent kinetics data.[48] While the quantum chemical and RRKM barriers are not directly comparable, it is likely that a multi-reference quantum chemical method would predict a barrier closer to the RRKM value.[50]

In a computational study of hydroxy-substituted isoprene radicals, Lei et al.[51] found no evidence for a barrier to O_2 addition. However, the reactions they studied have rate constants ∼10 times larger than the O_2 addition considered here. Also, in their study, Lei et al. did not look for authentic transition structures for O_2 addition, but instead performed a series of constrained optimizations at the B3LYP/3-21G(d) level.

According to the model chemistry predictions, formation of the vinoxy-O_2 adduct **10** is exothermic by −22 to −23 kcal/mol (Table 5). Transition structure **TS9** (Figure 3) is predicted to be rather early, with a C−C bond only 0.02 Å longer than in free vinoxy radical **4** (Figure 1b). This is consistent with the Hammond postulate[52] for exothermic reactions.

The chemically activated **10** can then isomerize either by abstracting the aldehydic H by a 1,4 shift (Reaction 18) or a methylene H by a 1,3 shift (Reaction 19).

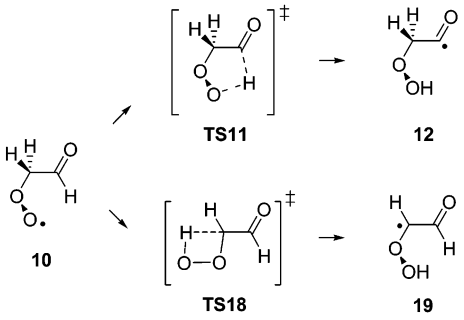

[18] [19]

All four quantum chemical methods predict that transition structure **TS11**, with the less strained five-member ring, is ∼20 kcal/mol lower in energy than transition structure **TS18** (Table 5). The torsional strain in **TS11** is somewhat relieved by a slight elongation of the C−C bond relative to reactant (**10**, Figure 3) and product (**12**, Figure 4).

Qualitatively, our quantum chemistry methods unambiguously predict that the chemically activated peroxy radical **10** will preferentially undergo a 1,4-hydrogen shift. Quantitatively, there are significant discrepancies among the four methods. MPW1K predicts a forward barrier for the 1,4-shift that is 6−7 kcal/mol higher than the other three methods, and B3LYP and MPW1K predict that the hydroperoxylacyl radical **12** is 4−5 kcal/mol less stable than do the model chemistries (Table 5). Moreover, the lengths of the breaking and forming bonds in transition structures **TS11** and **TS18** are notably different at the B3LYP/6-311G(2d,d,p) and QCISD/ 6-311G(d,p) levels (Table 6). While

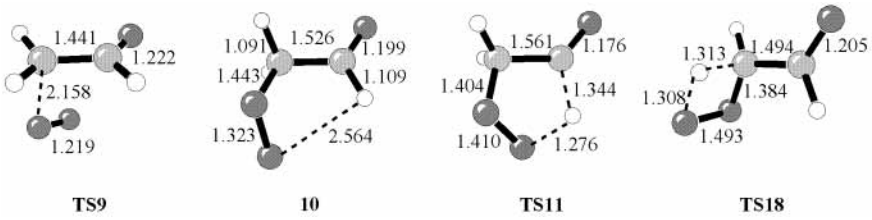

Figure 3. Formation and rearrangements of the vinoxylperoxy radical **10**. Bond lengths (in Å) computed at the B3LYP/6-311G(2d,d,p) level.

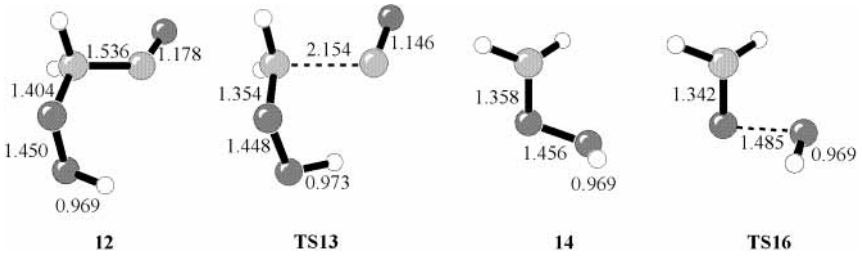

Figure 4. Decomposition of the hydroperoxylacyl radical **12**. Bond lengths (in Å) computed at the B3LYP/6-311G(2d,d,p) level.

TABLE 6: Breaking and Forming Bond Lengths (in Å) for the Hydrogen-Shift Transition Structures in Reactions 18 and 19

	geometry of **TS11**		geometry of **TS18**	
	r(C---H)	*r*(H---O)	*r*(C---H)	*r*(H---O)
B3LYP	1.347	1.269	1.312	1.305
CBS-QB3[a]	1.344	1.276	1.313	1.308
MPW1K	1.319	1.277	1.309	1.279
CBS-APNO[b]	1.321	1.290	1.322	1.281

[a] Uses B3LYP/6-311G(2d,d,p)-optimized geometries. [b] Uses QCISD/6-311G(d,p)-optimized geometries.

this discrepancy has no impact on the CBS-QB3 and CBS-APNO energy barriers predicted for the 1,4-hydrogen shift, the CBS-APNO barrier for the 1,3-hydrogen shift is 4 kcal/mol higher than the CBS-QB3 barrier. However, given the facility of the 1,4-shift, this difference has no impact on the chemistry predicted for the peroxy radical.

As a further test of our predictions for the chemically relevant 1,4-hydrogen shift, we applied Radom's CBS−RAD model chemistry[53] with QCISD/6-31G(d)-optimized geometries to species **10**, **TS11**, and **12**. The CBS−RAD method, which has been designed specifically to provide reliable energetics for radical species, predicts a forward barrier of 20.5 kcal/mol and a reverse barrier of 19.0 kcal/mol. These values agree to within 1 kcal/mol of the CBS-QB3 and CBS-APNO predictions. The fact that three rather different model chemistries predict essentially the same forward barrier gives us great confidence in this result.

C. Formation of a Second Equivalent of Hydroxy Radical. Our quantum chemical methods all predict that the hydroperoxylacyl radical **12** will fragment readily to generate •OH:

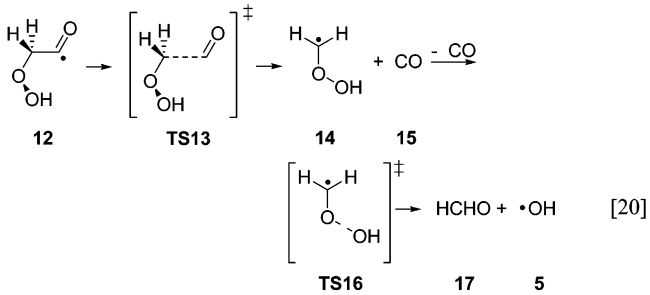

The lowest-barrier pathway starts with the slightly endothermic cleavage of the C−C bond to give carbon monoxide and the $\bullet CH_2OOH$ radical **14** (Figure 4). All methods besides MPW1K predict barriers of ∼10 kcal/mol (Table 5). Transition structure **TS13** is rather late, as expected from the Hammond postulate,[52] with a breaking C−C bond almost 2.2 Å long (Figure 4). Table 5 reveals that the density functional methods predict energies for the species in Reaction 20 all several kcal/mol higher than the model chemistry predictions. The origin of this difference may be that B3LYP and MPW1K both overestimate the stability of the vinoxylperoxy radical **10**, whose energy is the reference point in Table 5. This systematic error has already been noted for the radicals in Scheme 1 above and has been observed in other theoretical studies of peroxy[54] and sulfinyl[55] (RSO•) radicals. If this is the case, then B3LYP's correct prediction of the 1,4-hydrogen shift barrier in Reaction 18 is fortuitous: the method's tendency to underestimate transition-state energies happens to cancel its tendency to underestimate the energy of peroxy radicals.

The $\bullet CH_2OOH$ radical then undergoes β-scission to form formaldehyde and •OH. Although reactant **14** and transition structure **TS16** are authentic, distinct stationary points of the potential energy surface, all four methods predict (with zero-point energy corrections) that the transition structure, with an O−O bond only 0.03 Å longer than that of the reactant, is lower in energy than the reactant. The instability of such hydroperoxyalkyl radicals is well-established both experimentally and theoretically.[56,57] It is clear that **14** will fall apart immediately upon formation.[58]

D. Mechanistic and Atmospheric Implications. Our theoretical results clarify the mechanistic fates of ozonolysis intermediates. First, contrary to previous suggestions,[18] the decomposition of the parent vinyl hydroperoxide (Reaction 11) will occur more rapidly than its concerted rearrangement to hydroxyacetaldehyde (Reaction 12). Second, we provide a computational model for the chemistry of the vinoxylperoxy radical **10**. Its predominant unimolecular fate is abstraction of the aldehydic hydrogen (Reaction 18), as first proposed by Gutman and Nelson,[24] followed by stepwise fragmentation to •OH, H_2CO, and CO (Reaction 20). In Kroll et al's experiments,[20] this pathway will produce •OD radicals, along with CH_3CHO and CO.

The 1,4-hydrogen shift, which produces the labile hydroperoxy radical **12**, will compete with collisional stabilization of the chemically activated peroxy radical **10**. We have quantified this competition as a function of pressure by

TABLE 7: Yields of Collisionally Stabilized Peroxy (Y_{10}) and Labile Hydroperoxy (Y_{12}) Radicals as a Function of Pressure (in Torr)

	H-atom transfer		D-atom transfer	
pressure	Y_{10}	Y_{12}	Y_{10}	Y_{12}
1	0.00	1.00	0.00	1.00
10	0.01	0.99	0.01	0.99
50	0.10	0.90	0.17	0.83
100	0.26	0.74	0.33	0.67
200	0.42	0.58	0.52	0.48
400	0.60	0.40	0.72	0.28
760	0.75	0.25	0.82	0.18

performing RRKM/master equation calculations with Barker's MultiWell program.[47] Our calculations were based on the CBS-QB3 energies and the B3LYP/6-311G(2d,d,p) geometries and vibrational frequencies. We performed 1000 Monte Carlo trials at each pressure, giving yields reproducible to two decimal places. The activation energies of the entry and exit channels were varied by ±10% to determine the sensitivity of the results to these parameters. The exponential-down model for vibrational energy transfer was used, with the average energy transferred per collision ($\langle E_d \rangle$) assumed to be 300 cm^{-1}. This parameter was varied between 100 cm^{-1} and 1000 cm^{-1} to investigate the effects of this assumption.

Table 7 summarizes the predicted yields of peroxy versus hydroperoxy radical for both H and D transfer. Below 10 Torr, essentially all of the chemically activated **10** rearranges to form **12**. At 1 atm, stabilization of **10** dominates, but isomerization is still significant. As expected, substitution of D for H at the aldehydic position slows the atom transfer, thereby increasing the probability of collisional stabilization. However, the isotope effect is negligible at pressures below 10 Torr. Varying the activation energies and $\langle E_d \rangle$ as described above causes the 1-atm yield of hydroperoxy radical to vary from 0.1 to 0.4.

In their experiments on deuterated alkenes, Kroll et al.[20] report no primary kinetic isotope effect on hydroxy radical yields. This is consistent with our mechanism, since the rate-limiting step is the addition of O_2 to vinoxy radical (Reaction 17). However, under Kroll et al.'s experimental conditions (6 Torr), we predict that the yield of hydroperoxy radical from chemically activated peroxy radical should approach 100%. That is, half of the total hydroxy radical yield should come from the vinyl hydroperoxide (Reaction 7), and half from the vinoxy radical (Reaction 9). Since in Kroll et al.'s experiments, the vinoxylperoxy radicals are always deuterated at the aldehydic position, the relative yields of •OH and •OD (•OH:•OD) should be 1:1. However, the observed •OH:•OD ratios are 7:1 for *trans*-3-hexene and 2:1 for *cis*-3-hexene.

Several factors likely contribute to this discrepancy: (1) Since the CBS-QB3 barrier for the addition of O_2 to vinoxy radical is likely too high (as discussed above), the degree to which **10** is chemically activated is probably overestimated. This would decrease the yield of •OD at 6 Torr.[59] However, given the consensus among three different model chemical methods, we have great confidence that the barrier for the 1,4-hydrogen shift is (only) ~20 kcal/mol. (2) The energetics predicted here for the parent vinoxy radical will be somewhat different from the energetics for the 2-methylvinoxy radical generated in Kroll et al.'s experiments (Reaction 7). (3) Our simulations neglected tunneling, which would increase the predicted rate of •OH transfer, and therefore increase the predicted •OH:•OD ratio. (4) Other unimolecular reactions of the peroxy radical **10** may compete with the 1,4-hydrogen shift.

Nevertheless, our calculations provide strong evidence that syn carbonyl oxides are an important source of not only •OH, but also •OD, radicals in Kroll et al.'s experiments. The formation of •OH from decomposition of the vinyl hydroperoxide, and subsequent formation of •OD from the oxidation and isomerization of the vinoxy radical, is both mechanistically plausible and consistent with experiment.

Once thermalized, vinoxylperoxy radicals in the troposphere and in smog chamber experiments will undergo bimolecular reactions faster than they will isomerize. For example, the recommended rate constant for the reaction of •NO with the structurally similar acetonylperoxy radical ($CH_3C(O)CH_2O_2$•) is 8.0×10^{-12} cm^3 $molecule^{-1}$ s^{-1}.[60] For a typical tropospheric •NO mixing ratio of 1 ppb, the peroxy radical lifetime will be 5 s. In contrast, using our CBS-QB3 estimate of activation energy (19.5 kcal/mol) and a high-pressure-limit *A* factor of 1.6×10^{12} s^{-1} (derived from our master equation calculations), the vinoxylperoxy radical lifetime with respect to the 1,4-hydrogen shift is 2 min.

The self-reaction of the peroxy radicals is also likely to be important[61] and can lead to production of both hydroxyacetaldehyde **7** and glyoxal **20**, both of which have been observed in ozonolysis experiments.[16,48]

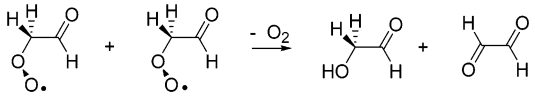

10 **10** **7** **20** [21]

This pathway to **7** is more likely than the rearrangement proposed in Reaction 12.

E. Comments on Quantum Chemical Methodology. Our results demonstrate the inconsistency of the B3LYP/6-31G(d,p) and MPW1K/6-31+G(d,p) methods as judged by model chemistry predictions and experimental thermochemical data. Fortuitously, B3LYP does not underestimate the barriers for the hydrogen-transfer reactions studied here and in fact dramatically overestimates the barriers for the 1,3-sigmatropic shifts in Reaction 12. MPW1K overestimates barriers both for Reaction 12 and the critical intramolecular 1,4-hydrogen shift in Reaction 18. Although MPW1K was optimized for hydrogen-transfer reactions, the training set involved intermolecular reactions of the form

$$\text{X-H} + \text{Y} \longrightarrow \left[\text{X---H---Y}\right]^{\ddagger} \longrightarrow \text{X} + \text{HY} \qquad [22]$$

where the X---H---Y angles were almost always 180°.[34] In contrast, transition structure **TS11** (Figure 3) is predicted to have an O---H---C angle of 129° at the B3LYP/6-311G(2d,d,p) level. Moreover, both B3LYP and MPW1K appear to overestimate the stability of certain radical species. Neither density functional method seems to provide reliable energetics for the systems considered here.[62]

The CBS-QB3 and CBS-APNO model chemistries predict relative energies that agree to within ±1 kcal/mol for most of the reactions of interest. This agreement comes despite some alarming differences in transition structure bond lengths, particularly for the 1,3-sigmatropic shifts (Table 4). If a particular simulation is quite sensitive to transition-state structure, the QCISD/6-311G(d,p)-optimized geometries employed in CBS-APNO are expected to be more reliable than the B3LYP/6-311G(2d,d,p)-optimized geometries employed by CBS-QB3.[30,32,34,37] However, for the master equation calculations employed here, such structural accuracy is not required. The

largest source of uncertainty in the yields reported in Table 7 is the energies, not the geometries or vibrational frequencies. Since the CBS-QB3 and CBS-APNO models give the same relative energies (to within chemical accuracy) for these systems, the more economical CBS-QB3 method is preferable. Moreover, given the large barriers predicted for O_2 addition to the vinoxy radical (Reaction 17), we should not presume that even CBS-APNO provides definitive energetics for this system.

IV. Conclusions

We provide quantum chemical evidence for the formation of hydroxy radicals from the reaction of vinoxy radicals with O_2. Under conditions in which prompt formation of •OH from the vinoxylperoxy radical is favorable, syn carbonyl oxides can generate two equivalents of •OH. Master equation simulations are necessary to quantify the extent to which carboxylic acids from anti carbonyl oxides also contribute to HO_x production in ozonolysis.

Preliminary calculations on the unimolecular reactions of syn propanal oxide indicate differences in activation barriers of ~2 kcal/mol. While this will not affect the qualitative conclusions of the present study, we are currently performing calculations to quantify the syn propanal oxide chemistry accurately. We are also exploring the role of vinoxy oxidation chemistry in the ozonolysis of other alkenes, and testing other quantum chemistry methods that may improve the accuracy of our simulations.

Acknowledgment. K.T.K. thanks the donors of the Petroleum Research Fund (#38037-GB6), administered by the American Chemical Society, and Macalester College (Wallace Research Grant) for support of this work. A.S.H. acknowledges support from the College of Science and Mathematics, California State University, Fresno. We thank R. G. Brisbois, K. N. Houk, B. J. Lynch, S. E. Paulson, and J. Zhang for useful discussions, and B. Koralesky and the National Computational Science Alliance facility at the University of Kentucky for computational expertise and resources.

References and Notes

(1) Paulson, S. E.; Orlando, J. J. *Geophys. Res. Lett.* **1996**, *23*, 3727.
(2) Hu, J.; Stedman, D. H. *Environ. Sci. Technol.* **1995**, *29*, 1655.
(3) Donahue, N. M.; Kroll, J. H.; Anderson, J. G.; Demerjian, K. L. *Geophys. Res. Lett.* **1998**, *25*, 59.
(4) Atkinson, R. *J. Phys. Chem. Ref. Data* **1997**, *26*, 215.
(5) Fenske, J. D.; Kuwata, K. T.; Houk, K. N.; Paulson, S. E. *J. Phys. Chem. A* **2000**, *104*, 7246.
(6) Rathman, W. C. D.; Claxton, T. A.; Rickard, A. R.; Marston, G. *Phys. Chem. Chem. Phys.* **1999**, *1*, 3981.
(7) Rickard, A. R.; Johnson, D.; McGill, C. D.; Marston, G. *J. Phys. Chem. A* **1999**, *103*, 7656.
(8) Gutbrod, R.; Schindler, R. N.; Kraka, E.; Cremer, D. *Chem. Phys. Lett.* **1996**, *252*, 221.
(9) Gutbrod, R.; Kraka, E.; Schindler, R. N.; Cremer, D. *J. Am. Chem. Soc.* **1997**, *119*, 7330.
(10) Anglada, J. M.; Bofill, J. M.; Olivella, S.; Solé, A. *J. Am. Chem. Soc.* **1996**, *118*, 4636.
(11) Niki, H.; Maker, P. D.; Savage, C. M.; Breitenbach, L. P.; Hurley, M. D. *J. Phys. Chem.* **1987**, *91*, 941.
(12) Zhang, D.; Lei, W.; Zhang, R. *Chem. Phys. Lett.* **2002**, *358*, 171.
(13) Zhang, D.; Zhang, R. *J. Am. Chem. Soc.* **2002**, *124*, 2692.
(14) Story, P. R.; Burgess, J. R. *J. Am. Chem. Soc.* **1967**, *89*, 5726.
(15) Story, P. R.; Burgess, J. R. *J. Am. Chem. Soc.* **1968**, *90*, 1094.
(16) Martinez, R. I.; Herron, J. T. *J. Phys. Chem.* **1987**, *91*, 946.
(17) Martinez, R. I.; Herron, J. T. *J. Phys. Chem.* **1988**, *92*, 4644.
(18) Grosjean, E.; Grosjean, D. *Atmos. Environ.* **1998**, *32*, 3393.
(19) Olzmann, M.; Kraka, E.; Cremer, D.; Gutbrod, R.; Andersson, S. *J. Phys. Chem. A* **1997**, *101*, 9421.
(20) Kroll, J. H.; Donahue, N. M.; Cee, V. J.; Demerjian, K. L.; Anderson, J. G. *J. Am. Chem. Soc.* **2002**, *124*, 8518.
(21) Cremer, D.; Kraka, E.; Szalay, P. G. *Chem. Phys. Lett.* **1998**, *292*, 97.
(22) Afeefy, H. Y.; Liebman, J. F.; Stein, S. E. Neutral Thermochemical Data; In *NIST Chemistry WebBook, NIST Standard Reference Database Number 69, March, 2003*; Linstron, P. J., Mallard, W. G., Eds.; National Institute of Standards and Technology: Gaithersburg, MD, 2003.
(23) Kroll, J. H.; Sahay, S. R.; Anderson, J. G.; Demerjian, K. L.; Donahue, N. M. *J. Phys. Chem. A* **2001**, *105*, 4446.
(24) Gutman, D.; Nelson, H. H. *J. Phys. Chem.* **1983**, *87*, 3902.
(25) Lorenz, K.; Rhäsa, D.; Zellner, R.; Fritz, B. *Ber. Bunsen-Ges. Phys. Chem.* **1985**, *89*, 341.
(26) Stephens, P. J.; Devlin, F. J.; Chabalowski, C. F.; Frisch, M. J. *J. Phys. Chem.* **1994**, *98*, 11623.
(27) Hehre, W. J.; Ditchfield, R.; Pople, J. A. *J. Chem. Phys.* **1972**, *56*, 2257.
(28) Hariharan, P. C.; Pople, J. A. *Theor. Chim. Acta* **1973**, *28*, 213.
(29) Montgomery, J. A.; Frisch, M. J.; Ochterski, J. W.; Petersson, G. A. *J. Chem. Phys.* **1999**, *110*, 2822.
(30) Chuang, Y.-Y.; Coitino, E. L.; Truhlar, D. G. *J. Phys. Chem. A* **2000**, *104*, 446.
(31) Fenske, J. D.; Hasson, A. S.; Paulson, S. E.; Kuwata, K. T.; Ho, A.; Houk, K. N. *J. Phys. Chem. A* **2000**, *104*, 7821.
(32) Coote, M. L.; Wood, G. P. F.; Radom, L. *J. Phys. Chem. A* **2002**, *106*, 12124.
(33) Lynch, B. J.; Fast, P. L.; Harris, M.; Truhlar, D. G. *J. Phys. Chem. A* **2000**, *104*, 4811.
(34) Lynch, B. J.; Truhlar, D. G. *J. Phys. Chem. A* **2001**, *105*, 2936.
(35) Kobayashi, Y.; Kamiya, M.; Hirao, K. *Chem. Phys. Lett.* **2000**, *319*, 695.
(36) Jursic, B. S. *J. Mol. Struct. Theochem.* **1998**, *430*, 17.
(37) Malick, D. K.; Petersson, G. A.; Montgomery, J. A., Jr. *J. Chem. Phys.* **1998**, *108*, 5704.
(38) Montgomery, J. A., Jr.; Ochterski, J. W.; Petersson, G. A. *J. Chem. Phys.* **1994**, *101*, 5900.
(39) Kang, J. K.; Musgrave, C. B. *J. Chem. Phys.* **2001**, *115*, 11040.
(40) Pople, J. A.; Head-Gordon, M.; Raghavachari, K. *J. Chem. Phys.* **1987**, *87*, 5968.
(41) Frisch, M. J.; Trucks, G. W.; Schlegel, H. B.; Scuseria, G. E.; Robb, M. A.; Cheeseman, J. R.; Zakrzewski, V. G.; Montgomery, J. A., Jr.; Stratmann, R. E.; Burant, J. C.; Dapprich, S.; Millam, J. M.; Daniels, A. D.; Kudin, K. N.; Strain, M. C.; Farkas, O.; Tomasi, J.; Barone, V.; Cossi, M.; Cammi, R.; Mennucci, B.; Pomelli, C.; Adamo, C.; Clifford, S.; Ochterski, J.; Petersson, G. A.; Ayala, P. Y.; Cui, Q.; Morokuma, K.; Malick, D. K.; Rabuck, A. D.; Raghavachari, K.; Foresman, J. B.; Cioslowski, J.; Ortiz, J. V.; Baboul, A. G.; Stefanov, B. B.; Liu, G.; Liashenko, A.; Piskorz, P.; Komaromi, I.; Gomperts, R.; Martin, R. L.; Fox, D. J.; Keith, T.; Al-Laham, M. A.; Peng, C. Y.; Nanayakkara, A.; Gonzalez, C.; Challacombe, M.; Gill, P. M. W.; Johnson, B.; Chen, W.; Wong, M. W.; Andres, J. L.; Gonzalez, C.; Head-Gordon, M.; Replogle, E. S.; Pople, J. A. *Gaussian 98*, Revision A.9; Gaussian, Inc.: Pittsburgh, PA, 1998.
(42) Bozzelli, J. W.; Sheng, C. *J. Phys. Chem. A* **2002**, *106*, 1113.
(43) Endo, Y.; Saito, S.; Hirota, E. *J. Chem. Phys.* **1985**, *83*, 2026.
(44) Dupuis, M.; Wendoloski, J. J.; Lester, W. A., Jr. *J. Chem. Phys.* **1982**, *76*, 488.
(45) Choi, J. Y.; Kim, C. K.; Kim, C. K.; Lee, I. *J. Phys. Chem. A* **2002**, *106*, 5709.
(46) Hasson, A. S.; Chung, M. Y.; Kuwata, K. T.; Converse, A. D.; Krohn, D.; Paulson, S. E. *J. Phys. Chem. A* **2003**, *107*, 6176.
(47) Barker, J. R. *Int. J. Chem. Kinet.* **2001**, *33*, 232.
(48) Zhu, L.; Johnston, G. *J. Phys. Chem.* **1995**, *99*, 15114.
(49) Oguchi, T.; Miyoshi, A.; Koshi, M.; Matsui, H.; Washida, N. *J. Phys. Chem. A* **2001**, *105*, 378.
(50) Lee's T_1 diagnostic (Lee, T. J.; Taylor, P. R. *Int. J. Quantum Chem. S.* **1989**, *23*, 199) applied to transition structure **TS9** gives a rather large value of 0.038, indicating that our single-reference methods may not provide a quantitatively accurate description of the addition of O_2. However, T_1 values for the other transition structures studied here are significantly lower, giving us general confidence in the reliability of our model chemistry reaction barriers.
(51) Lei, W.; Zhang, R.; McGivern, W. S.; Derecskei-Kovacs, A.; North, S. W. *J. Phys. Chem. A* **2001**, *105*, 471.
(52) Hammond, G. S. *J. Am. Chem. Soc.* **1955**, *77*, 334.
(53) Mayer, P. M.; Parkinson, C. J.; Smith, D. M.; Radom, L. *J. Chem. Phys.* **1998**, *108*, 604.
(54) Brinck, T.; Lee, H.-N.; Jonsson, M. *J. Phys. Chem. A* **1999**, *103*, 7094.
(55) Gregory, D. D.; Jenks, W. S. *J. Org. Chem.* **1998**, *63*, 3859.
(56) Sumathi, R.; Green, W. H., Jr. *Phys. Chem. Chem. Phys.* **2003**, *5*, 3402.
(57) Niki, H.; Maker, P. D.; Savage, C. M.; Breitenbach, L. P. *J. Phys. Chem.* **1983**, *87*, 2190.
(58) Along these lines, we found on the B3LYP surface a concerted transition structure (not shown) in which the C−C and O−O bonds of **12** cleave simultaneously to give H_2CO, CO, and •OH. However, CBS-QB3 predicts this transition structure to be 7.4 kcal/mol higher in energy than **TS13**.

(59) Interestingly, in their experimental study of vinoxy oxidation, Lorenz et al. (ref 25) report a •OH yield of 20% at ~20 Torr. However, this result was not corrected for secondary reactions that would decrease the observed •OH yield.

(60) Tyndall, G. S.; Cox, R. A.; Granier, C.; Lesclaux, R.; Moortgat, G. K.; Pilling, M. J.; Ravishankara, A. R.; Wallington, T. J. *J. Geophys. Res.* **2001**, *106*, 12157.

(61) Under NO_x-free conditions, assuming that the concentration of vinoxylperoxy radicals in smog chamber experiments is $\sim 10^{11}$ molecule cm^{-3}, and estimating a vinoxylperoxy self-reaction rate of 2×10^{-12} cm^3 $molecule^{-1}$ s^{-1} (Kirchner, F.; Stockwell, W. R. *J. Geophys. Res.* **1996**, *101*, 21007), the peroxy radical lifetime should be 5 s.

(62) Radom and co-workers (ref 32) have recently expressed reservations about MPW1K's treatment of $\bullet CH_3$-transfer reactions.